ELSEVIER

Journal of Alloys and Compounds 229 (1995) 248–253

Journal of ALLOYS AND COMPOUNDS

Hydrogen in the A15 compounds Nb_3Sn and Nb_3Al: a nuclear magnetic resonance study

A.V. Skripov, M.Yu. Belyaev, V.E. Arkhipov

Institute of Metal Physics, Urals Branch of the Academy Sciences, Ekaterinburg 620219, Russian Federation

Received 22 December 1994; in final form 24 April 1994

Abstract

Nuclear magnetic resonance measurements of the ^{119}Sn, ^{27}Al Knight shifts and the ^{119}Sn, ^{27}Al and ^{1}H spin–lattice relaxation rates in the A15-type compounds $Nb_3SnH_x(D_x)$ ($x = 0$, 0.7 and 1.2) and Nb_3AlH_x ($x = 0$, 2.3) have been performed over the temperature range 10–460 K. The low temperature ^{119}Sn Knight shift and spin–lattice relaxation data indicate that in $Nb_3SnH_x(D_x)$ the density of electron states at the Fermi level decreases strongly with increasing x. The hydrogen mobility in Nb_3Al is found to be much higher than that in Nb_3Sn. The behaviour of the proton spin–lattice relaxation rate for $Nb_3AlH_{2.3}$ in a wide range of resonance frequencies (9–90 MHz) can be described by the model using a double-peak distribution of activation energies.

Keywords: Diffusion; Nuclear magnetic resonance; Hydrogen

1. Introduction

The intermetallic compounds Nb_3Sn and Nb_3Al belong to the family of A15-type superconductors showing a number of unusual physical properties [1]. Some of the A15 compounds are known to absorb large amounts of hydrogen [2–7]. The host lattice usually retains the A15 structure after hydrogen absorption. Previous studies of the effects of hydrogen in A15 compounds were devoted mainly to its impact on the superconducting transition temperature T_c [2–4,8,9]. However, little is known about hydrogen mobility in these compounds and hydrogen-induced changes in the electronic structure. Microscopic information on these properties can be obtained from nuclear magnetic resonance (NMR) experiments. Proton NMR studies of H mobility have been reported for the A15-type hydrides Ti_3IrH_x [10], Ti_3SbH_x [11] and V_3GaH_x [12]. The aim of the present work is to investigate the electronic properties and hydrogen diffusion in the systems Nb_3Sn–H(D) and Nb_3Al–H using ^{119}Sn, ^{27}Al and ^{1}H NMR measurements.

According to the neutron diffraction data [8], H atoms in $Nb_3SnH_{1.0}$ occupy only the sixfold d positions of the space group $Pm\bar{3}n$, i.e. the tetrahedral interstitial sites (formed by four Nb atoms) on the faces of the unit cell. The occupation of d sites has been confirmed by recent neutron diffraction measurements on the deuteride $Nb_3SnD_{0.7}$ [13]. The value of T_c in Nb_3SnH_x is found to decrease strongly with increasing hydrogen content [8,14], being below 4.2 K for $x \geq 0.6$. The heat capacity studies of Nb_3SnH_x [14] have shown that the electronic specific heat coefficient decreases with increasing x. For Nb_3AlH_x system, two phases with the A15-type host lattice but with different lattice parameters are found to coexist in the concentration range $0.2 \leq x \leq 1.5$ [15]. The hydride phase of Nb_3AlH_x ($x \geq 1.5$) is not superconducting above 2 K [15]. To the best of our knowledge, there is no direct information on the positions occupied by hydrogen in Nb_3Al. However, the occupation of d sites seems to be most probable. This would be consistent with the chemical affinity model [16] predicting the preferential occupation of interstices surrounded by a larger number of hydride-forming elements (in our case, Nb) and with the general trends observed for many hydrides of intermetallic compounds [17].

0925-8388/95/$09.50 © 1995 Elsevier Science S.A. All rights reserved
SSDI 0925-8388(95)01692-9

2. Experimental details

The Nb_3Sn samples were prepared by sintering compacted Nb and Sn powders as described in Ref. [18]. According to the X-ray diffraction analysis, in addition to the main phase with the A15-type structure the sample contained also about 5% of extra phases (mainly b.c.c. Nb). The superconducting transition temperature measured by induction method was 17.0 K. Nb_3Al samples were prepared by arc melting appropriate amounts of Nb and Al in argon atmosphere. The amount of extra phases in this sample was found to be less than 5% and $T_c = 17.8$ K.

The samples were charged with H_2 (D_2) gas at a pressure of about 1 bar using a Sieverts-type vacuum system. The H (D) content was determined from the hydrogen pressure change in the calibrated volume of the system. Charging of Nb_3Sn with the light H isotope resulted in the composition $Nb_3SnH_{1.2}$. However, for deuterium in Nb_3Sn under the same conditions, it was only possible to attain the composition $Nb_3SnD_{0.7}$. Nb_3Al readily absorbs larger amounts of hydrogen; measurements were made on the sample of $Nb_3AlH_{2.3}$. All these hydrided samples are not superconducting above 4.2 K. X-ray diffraction analysis has shown that the main phase of the hydrided samples retains the A15-type structure of the host lattice, the amount of extra phases being approximately the same as in the hydrogen-free materials. The lattice parameters of the A15 phase are listed in Table 1. Our structural data are consistent with the results of previous experiments [8,14,15].

NMR measurements were performed on a Bruker SXP pulse spectrometer at the frequencies $\omega/2\pi =$ 32 MHz (^{119}Sn), 21 MHz (^{27}Al) and 9, 18 and 90 MHz (^{1}H). ^{119}Sn and ^{27}Al NMR spectra were recorded by integrating the echo signal and sweeping the magnetic field. Spin–lattice relaxation times T_1 were determined from the recovery of the echo signal after the saturation pulse sequence (^{119}Sn and ^{27}Al) and from the recovery of the free-induction decay (FID) signal after inverting r.f. pulse (^{1}H).

3. Results and discussion

3.1. ^{119}Sn and ^{27}Al Knight shifts and spin–lattice relaxation rates

For both ^{119}Sn in Nb_3Sn and ^{27}Al in Nb_3Al the NMR spectrum consists of a single symmetric line, as expected for sites having cubic point symmetry. In hydrided compounds the line becomes broader owing to a random occupation of interstitial sites, resulting in distributions of magnetic dipolar fields and electric field gradients at Sn and Al sites. We have found, however, that the additional broadening of the low temperature ^{119}Sn lines in $Nb_3SnD_{0.7}$ and $Nb_3SnH_{1.2}$ is small, the line shapes being nearly symmetric. This is consistent with the occupation of d sites by H (D) atoms, since these sites have no nearest-neighbour Sn sites. The values of the ^{119}Sn and ^{27}Al Knight shifts measured at 20 K are presented in Table 1. The results for hydrogen-free compounds Nb_3Sn and Nb_3Al are in a good agreement with previous measurements [19]. It can be seen that the absolute value of K_{Sn} strongly decreases with increasing x. On the other hand, the value of K_{Al} remains nearly unchanged after the hydrogen absorption.

The spin–lattice relaxation of both ^{119}Sn and ^{27}Al in all samples can be fitted by a single-exponential function. In the temperature ranges studied (20–40 K for hydrogen-free samples and 10–40 K for hydrided compounds) the spin–lattice relaxation rates $(T_1^{-1})_{Sn}$ and $(T_1^{-1})_{Al}$ are found to be proportional to temperature, as expected for the electronic (Korringa) contribution to the relaxation rate. Hydrogen hopping is frozen on the NMR frequency scale in this temperature range, so that the measured rates $(T_1^{-1})_{Sn,Al}$ are not affected by H (D) jumps. The values of $[(T_1T)^{-1}]_{Sn}$ and $[(T_1T)^{-1}]_{Al}$ are listed in Table 1. For the hydrogen-free Nb_3Al the value of $[(T_1T)^{-1}]_{Al}$ is in a good agreement with the results of previous measurements [19,20]. As can be seen from Table 1, for both Nb_3Sn and Nb_3Al, hydrogen absorption results

Table 1
Lattice parameters, magnetic susceptibilities and the low temperature values of ^{119}Sn and ^{27}Al Knight shifts and spin–lattice relaxation rates for $Nb_3SnH_x(D_x)$ and Nb_3AlH_x (estimated errors in the last digit are given in parentheses).

Sample	a_0 (Å)	χ(295 K) ($\times 10^{-4}$ emu mol^{-1})	K_{Sn} (%)	K_{Al} (%)	$[(T_1T)^{-1}]_{Sn}$ (s^{-1} K^{-1})	$[(T_1T)^{-1}]_{Al}$ (s^{-1} K^{-1})
Nb_3Sn	5.289(1)	6.99(3)	−0.40(1)		4.10(8)	
$Nb_3SnD_{0.7}$	5.324(1)	5.36(3)	−0.07(1)		0.33(2)	
$Nb_3SnH_{1.2}$	5.350(1)	3.39(2)	−0.01(1)		0.087(4)	
Nb_3Al	5.189(2)			0.01(1)		0.077(4)
$Nb_3AlH_{2.3}$	5.317(2)			0.02(1)		0.047(3)

in the decrease in the relaxation rate which is especially pronounced for Nb_3Sn.

In transition metal compounds the Knight shift at nuclear sites of p atoms usually consists of two main contributions:

$$K = K_s + K_d = \frac{1}{\mu_B N_A}(H_s\chi_s + H_d\chi_d) \quad (1)$$

where K_s is the contact contribution due to s electrons, K_d is the core polarization spin contribution of d electrons, χ_s and χ_d are the spin susceptibilities of s and d electrons respectively, H_s and H_d are the appropriate hyperfine fields at nuclear sites, μ_B is the Bohr magneton and N_A is the Avogadro number. In a first approximation the spin susceptibilities χ_s and χ_d are proportional to the corresponding densities $N_s(E_F)$ and $N_d(E_F)$ of electron states at the Fermi level. The value of $N_d(E_F)$ is usually much higher than that of $N_s(E_F)$, i.e. $\chi_d \gg \chi_s$. While the contact hyperfine field H_s is always positive, the core polarization hyperfine field H_d is typically negative (i.e. antiparallel to the external magnetic field). Our results show that for ^{119}Sn in Nb_3Sn the second term in Eq. (1) is dominant. The observed changes in K_{Se} with H(D) content suggest that in $Nb_3SnH_x(D_x)$ the value of $N_d(E_F)$ strongly decreases with increasing x. This is consistent with the heat capacity data for Nb_3SnH_x [14] and with the results of our magnetic susceptibility measurements included in Table 1. For ^{27}Al in Nb_3Al the positive and negative contributions to the Knight shift nearly compensate each other. The absence of any significant changes in K_{Al} after hydrogen absorption suggests that such an approximate compensation is retained also for $Nb_3AlH_{2.3}$.

The low temperature spin–lattice relaxation rate also results from the sum of two main contributions:

$$(T_1T)^{-1} = [(T_1T)^{-1}]_s + [(T_1T)^{-1}]_d = 2h\gamma^2k_B[H_s^2N_s^2(E_F) + qH_d^2N_d^2(E_F)] \quad (2)$$

where γ is the nuclear gyromagnetic ratio and q is the dimensionless reduction factor ($0 \leq q \leq 1$) [21]. Since $(T_1T)^{-1}$ contains only terms proportional to the squares of the partial densities of electron states at the Fermi level, the relaxation rate is expected to give more direct information on the changes in $N(E_F)$ than the Knight shift. The $[(T_1T)^{-1}]_{Sn}$ results for $Nb_3SnH_x(D_x)$ are consistent with a considerable decrease in $N(E_F)$ with increasing x. Assuming that the hyperfine fields at Sn sites are nearly constant in the studied range of x, we can estimate the relative changes in $N(E_F)$ for $Nb_3SnH_x(D_x)$ using the low temperature $[T_1T)^{-1}]_{Sn}$ data. The upper limits of $N(E_F)$ values for $Nb_3SnD_{0.7}$ and $Nb_3SnH_{1.2}$ are found to be equal to 28% and 15% respectively, of the $N(E_F)$ value for Nb_3Sn. A strong reduction in $N(E_F)$ with increasing hydrogen content is also typical of the other A15 compounds with a narrow $N_d(E)$ peak near the Fermi level [11,12,22]. The interpretation of the $[(T_1T)^{-1}]_{Al}$ data for Nb_3AlH_x appears to be not so straightforward. It should be noted that the value of $[(T_1T)^{-1}]_{Al}$ for Nb_3Al is unusually small, being approximately a seventh of the $[(T_1T)^{-1}]_{Al}$ value for aluminium metal. This implies that the hyperfine fields at Al sites and/or the densities of electron states at the Fermi level in Nb_3Al are very low. The estimates based on the Korringa-like relations for both the contact and the core polarization contributions to K_{Al} and $[(T_1T)^{-1}]_{Al}$ show that the relaxation rate in Nb_3Al is dominated by the contact interaction [19]. The observed effects of hydrogen absorption on K_{Al} and $[(T_1T)^{-1}]_{Al}$ can be qualitatively accounted for, if we assume that $N_s(E_F)$ decreases and $N_d(E_F)$ increases with increasing x.

3.2. ^1H spin–lattice relaxation rates

The proton FID in our $Nb_3SnH_{1.2}$ sample at $T \geq 190$ K is found to consist of two components. The long FID component corresponding to mobile protons on the NMR frequency scale has a small amplitude (about 5% of the total FID amplitude at 295 K). This component originates from protons in the additional phase, β-NbH_x. We have verified this by Fourier transforming the long FID component and observing the characteristic change in the line shape due to the $\alpha \rightarrow \beta$ transition at $T \approx 390$ K. All results to be discussed below correspond to the short FID component originating from protons in the main A15 phase. For $Nb_3AlH_{2.3}$ the proton FID is one component in the entire temperature range studied.

The measured proton spin–lattice relaxation rate in metal–hydrogen systems usually results from the sum of the contribution (T_{1e}^{-1}) due to the hyperfine interactions with conduction electrons and the contribution T_{1d}^{-1} due to the dipole–dipole interactions modulated by hydrogen motion:

$$(T_1^{-1})_H = (T_{1e}^{-1})_H + (T_{1d}^{-1})_H. \quad (3)$$

The electronic (Korringa) term is typically proportional to temperature, $T_{1e}^{-1} = CT$, and does not depend on ω. This term is expected to dominate at low temperatures. According to the Bloembergen–Purcell–Pound (BPP) [23] theory of motional relaxation, T_{1d}^{-1} should have a maximum at the temperature T_{max} at which the condition $\omega\tau_d \approx 1$ is satisfied, τ_d being the mean dwell time of the H atom in an interstitial site. At high temperatures ($\omega\tau_d \ll 1$), $T_{1d}^{-1} \propto \tau_d$ and, at low temperatures ($\omega\tau_d \gg 1$),

$T_{1d}^{-1} \propto \omega^{-2}\tau_d^{-1}$. Lattice-specific Monte Carlo calculations of T_{1d}^{-1} [24] lead to results that are close to the BPP predictions. In particular, the asymptotic behaviour of T_{1d}^{-1} in the high temperature and low temperature limits appears to be the same as in the BPP model. If τ_d follows the Arrhenius relation, $\tau_d = \tau_{d0}\exp(E_a/k_BT)$, where E_a is the activation energy for hydrogen diffusion, then a plot of $\log T_{1d}^{-1}$ vs. T^{-1} is expected to be linear in both the high temperature and the low temperature limits with the slopes E_a/k_B and $-E_a/k_B$ respectively.

Fig. 1 shows the temperature dependence of the proton spin–lattice relaxation rate in $Nb_3SnH_{1.2}$ measured at 90 MHz. The low temperature proton T_1^{-1} data for $Nb_3AlH_{2.3}$ at 90 MHz are also included for comparison. It can be seen that in $Nb_3AlH_{2.3}$ the relaxation rate shows the expected Korringa behaviour at low T with $C = [(T_{1e}T)_H]^{-1} = 5.7 \times 10^{-3}\ s^{-1}\ K^{-1}$. The rapid growth of T_1^{-1} above 150 K is due to the motional contribution (T_{1d}^{-1} term) which goes through a maximum at higher T. In contrast, the temperature dependence of the proton T_1^{-1} in $Nb_3SnH_{1.2}$ shows deviations from the Korringa behaviour at low T. In fact, the extrapolation of the measured $T_1^{-1}(T)$ dependence for this sample to $T = 0$ results in a finite value of the relaxation rate. This feature may originate from the effects of paramagnetic impurities [25] and/or from the mechanism of cross-relaxation between proton and quadrupolal nuclear spins [26]. The onset of the growth of T_1^{-1} related to the motional contribution in $Nb_3SnH_{1.2}$ occurs at a much higher temperature than in $Nb_3AlH_{2.3}$. This means that hydrogen motion in $Nb_3SnH_{1.2}$ is much slower than in $Nb_3AlH_{2.3}$. The origin of such a strong difference between the hydrogen mobilities of these two related compounds remains to be elucidated. For $Nb_3SnH_{1.2}$ the expected relaxation rate maximum should occur outside the temperature range of the present measurements; therefore it is difficult to estimate motional parameters of H in this compound reliably. The behaviour of the proton FID indicates that the hopping rate of H atoms in $Nb_3SnH_{1.2}$ is lower than $5 \times 10^4\ s^{-1}$ at $T \leq 380$ K.

For $Nb_3AlH_{2.3}$ the proton spin–lattice relaxation results show clear effects of H motion at $T \geq 180$ K. In order to obtain a better characterization of the motion, at $T \geq 220$ K we have measured T_1^{-1} in this compound at three resonance frequencies: 9, 18 and 90 MHz. The motional contribution T_{1d}^{-1} is determined by subtracting T_{1e}^{-1} from the measured T_1^{-1} values. Fig. 2 shows the temperature dependence of T_{1d}^{-1} at three frequencies. It can be seen that the experimental data exhibit strong deviations from the predictions of the BPP theory. In particular, the low temperature slope of the $\log T_{1d}^{-1}$ vs. T^{-1} plots is less steep than the high temperature slope, and the frequency dependence of T_{1d}^{-1} at low temperatures is weaker than ω^{-2}. These features are often observed for hydrogen in alloys and intermetallic compounds; in many cases they can be accounted for by the model employing a distribution of τ_d (or E_a) values [27,28]. We have found, however, that the BPP model with a single-peak Gaussian distribution of E_a values fails to give a reasonable description of our data at all the frequencies studied. In particular, this model does not allow us to describe at the same time the strong difference between the high T and low T slopes of the

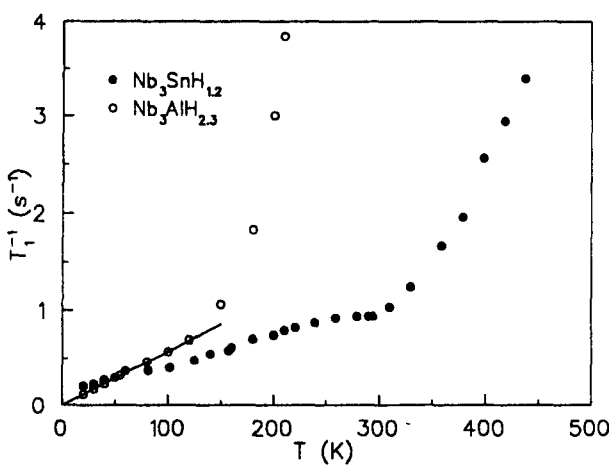

Fig. 1. Temperature dependence of the proton spin–lattice relaxation rate in $Nb_3SnH_{1.2}$ and $Nb_3AlH_{2.3}$ measured at 90 MHz. The line shows the linear fit to the low temperature data for $Nb_3AlH_{2.3}$.

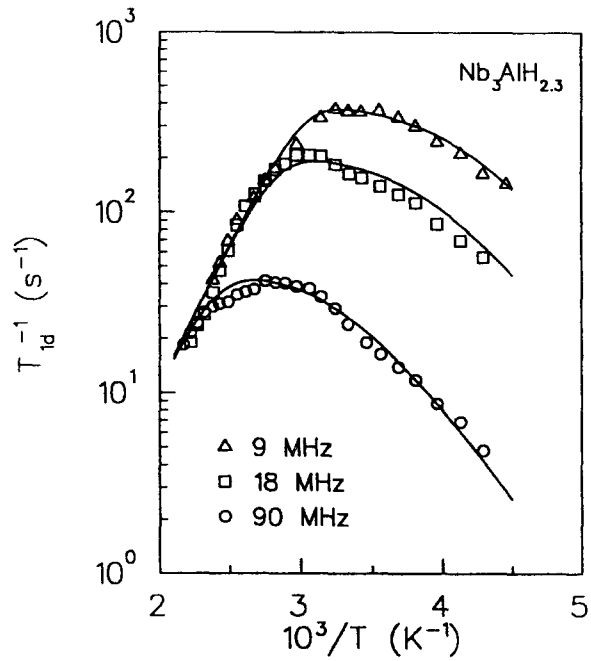

Fig. 2. Motional contributions to the proton spin–lattice relaxation rate in $Nb_3AlH_{2.3}$ at 9, 18 and 90 MHz as functions of reciprocal temperature. The lines represent the fit of the double-peak model of E_a distribution to the data (see text for details).

log T_{1d}^{-1} vs. T^{-1} plots and the disappearance of the frequency dependence of T_{1d}^{-1} at temperatures only slightly exceeding T_{max}. Therefore we use the BPP model with a normalized double-peak distribution of E_a values:

$$G(E_a) = (1 - A)G_1(E_a, \overline{E}_{a1}, \Delta E_{a1}) + AG_2(E_a, \overline{E}_{a2}, \Delta E_{a2}) \quad (4)$$

where $\overline{E}_{a1}$ and $\overline{E}_{a2}$ are the average activation energies, and ΔE_{a1} and ΔE_{a2} are the distribution widths for two peaks. This model has earlier been found to give a good fit to the proton spin relaxation data for the C15-type $ZrTi_2H_x$ in a very wide frequency range [29]. As for $ZrTi_2H_x$, we assume that the width ΔE_{a1} of the high E_a peak centred on $\overline{E}_{a1}$ is negligible, i.e. $G_1(E_a, \overline{E}_{a1}, \Delta E_{a1}) \approx \delta(E_a - \overline{E}_{a1})$. This assumption is consistent with the observed rapid disappearance of the frequency dependence of T_{1d}^{-1} above T_{max}. For G_2 we choose the Gaussian shape. The variable parameters are the values of τ_{d0}, A, $\overline{E}_{a1}$, $\overline{E}_{a2}$, ΔE_{a2} and the "rigid-lattice" second moments of the proton NMR line due to H–H and metal–H dipolar interactions. We look for a set of parameters giving the best fit to the $T_{1d}^{-1}(T)$ data at three frequencies simultaneously. The results of this fitting procedure are shown as lines in Fig. 2, the fitting parameters being $\overline{E}_{a1} = 0.32$ eV, $\overline{E}_{a2} = 0.27$ eV, $\Delta E_{a2} = 0.03$ eV (full width at half-maximum), $\tau_{d0} = 1.6 \times 10^{-13}$ s and $A = 0.70$. As can be seen from Fig. 2, the model gives a satisfactory description of the $T_{1d}^{-1}(T)$ data at three frequencies with the same set of parameters.

The model using a double-peak distribution of E_a implies the coexistence of two different frequency scales of H hopping. In our case the low E_a peak centred on $\overline{E}_{a2}$ appears to be dominant ($A = 0.70$). The other (high E_a) peak corresponding to slower hopping has a lower intensity. This is typical of systems with hydrogen trapping [30] where the slower frequency scale corresponds to the detrapping rate τ_{d1}^{-1} of hydrogen atoms from "deep" sites and the faster scale is related to the hydrogen hopping rate τ_{d2}^{-1} between "shallow" sites. It should be noted that the motional contribution to the proton spin–lattice relaxation rate in $Nb_3AlH_{2.3}$ is dominated by ^{93}Nb–^1H dipolar interactions. This means that microscopic field fluctuations at a proton site are determined mainly by hopping of this proton itself, rather than by hopping of its neighbours. In the high temperature region where $\omega\tau_{d1} \ll 1$ and $\omega\tau_{d2} \ll 1$ the measured relaxation rate is insensitive to details of individual jumps, being determined by an average over many jumps, including trapping and detrapping. At lower temperatures the escape processes from "deep" sites and the hopping between "shallow" sites may be resolved; they are expected to result in the relaxation rate maxima at two different temperatures corresponding to the conditions $\omega\tau_{d1} \approx 1$ and $\omega\tau_{d2} \approx 1$ respectively. In our case these maxima are not resolved, being quite close to each other. In systems with larger difference between τ_{d1} and τ_{d2}, such as NbO_yH_x [30] and $ZrMo_2H_{1.2}$ [31], the relaxation rate maxima due to different jump processes are partially resolved. The existence of a τ_d distribution for a particular jump process may be attributed to the dependence of the jump rate on the configuration of neighbouring H atoms. Such a description is equivalent to the two-state model [32] which is often used for interpretation of quasi-elastic neutron scattering data in the hydrides of alloys and intermetallic compounds. The nature of inequivalent sites in our $Nb_3AlH_{2.3}$ sample is not clear yet. One may expect that in concentrated A15 hydrides H atoms occupy in addition to d sites some other types of site. The occupation of both d and k positions by D atoms has been recently found in the A15-type $Ti_3IrD_{3.6}$ [13]. The other possibility is that the trapping interstitial sites are formed owing to antisite defects in the host lattice.

Motional parameters resulting from the fit of the proton T_{1d}^{-1} data to the double-peak model appear to be quite reasonable. The value of τ_{d0} is within the range 10^{-14}–10^{-12} s typical of hydrogen in metals. The small value of $\overline{E}_{a1} - \overline{E}_{a2} = 0.05$ eV indicates that the difference between site energies of H in "deep" and "shallow" sites is not large, and both types of site are likely to be occupied with considerable probability. The average activation energy $\overline{E}_{a2}$ for the long-range H diffusion in $Nb_3AlH_{2.3}$ is comparable with that in the concentrated A15-type hydride Ti_3IrH_x (for $x = 3.5$, $E_a = 0.265 \pm 0.020$ eV [10]).

4. Conclusions

The main results of our ^{119}Sn, ^{27}Al and ^1H NMR measurements in the A15-type systems Nb_3Sn–H(D) and Nb_3Al–H may be summarized as follows.

The density of electron states at the Fermi level in $Nb_3SnH_x(D_x)$ decreases strongly with increasing x. Such behaviour is typical for the A15 compounds with a narrow $N(E)$ peak near the Fermi level. For the Nb_3Al–H system the dependence of $N(E_F)$ on the H concentration appears to be much weaker. This may be related to the low value of $N(E_F)$ in the hydrogen-free Nb_3Al.

Proton spin–lattice relaxation rate measurements have shown that hydrogen mobility in Nb_3Al is much higher than in Nb_3Sn. The behaviour of the proton relaxation rate in $Nb_3AlH_{2.3}$ can be described by the model using a double-peak distribution of activation energies. This suggests that H atoms in $Nb_3AlH_{2.3}$ occupy at least two types of site.

Acknowledgments

We are grateful to K.N. Mikhalev for the magnetic susceptibility measurements. The research described in this paper was made possible in part by Grant NMJ000 from the International Science Foundation. A.V.S. is grateful to the Alexander von Humboldt Foundation for a Research Fellowship.

References

[1] S.V. Vonsovsky, Yu. A. Izyumov and E.Z. Kurmaev, *Superconductivity of Transition Metals, Their Alloys and Compounds*, Springer, Berlin, 1982.
[2] P.R. Sahm, *Phys. Lett. A, 26* (1968) 459.
[3] S.Z. Huang, T. Skoskiewicz, C.W. Chu and J.L. Smith, *Phys. Rev. B, 22* (1980) 137.
[4] V.E. Antonov, T.E. Antonova, I.T. Belash, O.V. Zharikov, A.I. Latynin, A.V. Palnichenko and V.I. Rashchupkin, *Sov. Phys.–Solid State, 31* (1989) 1659.
[5] K.V.S. Rama Rao, M. Mrowietz and A. Weiss, *Ber. Bunsenges. Phys. Chem., 86* (1982) 1135.
[6] M. Schlereth and H. Wipf, *J. Phys.: Condens. Matter, 2* (1990) 6927.
[7] M. Baier, R. Wordel, F.E. Wagner, T.E. Antonova and V.E. Antonov, *J. Less-Common Met., 172* (1991) 358.
[8] L.J. Vieland, A.W. Wicklund and J.G. White, *Phys. Rev. B, 11* (1975) 3311.
[9] K.V.S. Rama Rao, H. Sturm, B. Elschner and A. Weiss, *Phys. Lett. A, 93* (1983) 492.
[10] D. Guthardt, D. Beisenherz and H. Wipf, *J. Phys.: Condens. Matter, 4* (1992) 6919.
[11] A.V. Skripov, M. Yu. Belyaev and S.A. Petrova, *J. Phys.: Condens. Matter, 4* (1992) *L*537.
[12] A.V. Skripov, Yu.G. Cherepanov and H. Wipf, *J. Alloys Comp, 209* (1994) 111.
[13] K. Cornell, U. Stuhr, H. Wipf, N. Stüsser and A.V. Skripov, to be published.
[14] V. Shamrai, K. Bohmhammel and G. Wolf, *Phys. Status Solidi B, 109* (1982) 511.
[15] V.F. Shamrai and L.N. Padurets, *Dokl. Acad. Nauk SSSR, 246* (1979) 1182.
[16] I. Jacob and D. Shaltiel, *J. Less-Common Met., 65* (1979) 117.
[17] K. Yvon and P. Fischer, in L. Schlapbach (ed.), *Hydrogen in Intermetallic Compounds I*, Springer, Berlin, 1988, p. 87.
[18] A.E. Karkin, V.E. Arkhipov, B.N. Goshchitskii, E.P. Romanov and S.K. Sidorov, *Phys. Status Solidi A, 38* (1976) 433.
[19] E. Ehrenfreund, A.C. Gossard and J.H. Wernick, *Phys. Rev. B, 4* (1971) 2906.
[20] A.V. Skripov and A.P. Stepanov, *Sov. J. Low Temp. Phys., 5* (1979) 32.
[21] A. Narath, in A.J. Freeman and R.B. Frankel (eds.), *Hyperfine Interactions*, Academic, New York, 1967, p. 287.
[22] B. Cort, G.R. Stewart, S.Z. Huang, R.L. Meng and C.W. Chu, *Phys. Rev. B, 24* (1981) 5058.
[23] N. Bloembergen, E.M. Purcell and R.M. Pound, *Phys. Rev., 73* (1948) 679.
[24] D.A. Faux, D.K. Ross and C.A. Sholl, *J. Phys. C: Solid State Phys., 19* (1986) 4115.
[25] T.T. Phua, B.J. Beaudry, D.T. Peterson, D.R. Torgeson, R.G. Barnes, M. Belhoul, G.A. Styles and E.F.W. Seymour, *Phys. Rev. B, 28* (1983) 6227.
[26] L.R. Lichty, J.W. Han, D.R. Torgeson, R.G. Barnes and E.F.W. Seymour, *Phys. Rev. B, 42* (1990) 7734.
[27] J. Shinar, D. Davidov and D. Shaltiel, *Phys. Rev. B, 30* (1984) 6331.
[28] J.T. Markert, E.J. Cotts and R.M. Cotts, *Phys. Rev. B, 37* (1988) 6446.
[29] A.V. Skripov, S.V. Rychkova, M.Yu. Belyaev and A.P. Stepanov, *Solid State Commun., 71* (1989) 1119.
[30] R. Messer, A. Blessing, S. Dais, D. Höpfel, G. Majer, C. Schmidt, A. Seeger, W. Zag and R. Lässer, *Z. Phys. Chem. N.F., Suppl. 2* (1986) 61.
[31] W. Renz, G. Majer and A.V. Skripov, to be published.
[32] D. Richter and T. Springer, *Phys. Rev. B, 18* (1978) 126.